

PHOTOINDUCED ELECTRON TRANSFER FROM AROMATIC AMINES TO TRIPLET STATES OF C₆₀

YUKIO YAHATA, YOSHIKO SASAKI,[†] MAMORU FUJITSUKA AND OSAMU ITO[†]
Institute for Chemical Reaction Science, Tohoku University, Katahira, Sendai 980-77, Japan,
[†]Shokei Girl's High School, Hirose-machi, Aoba-ku, Sendai 980, Japan

(Received 28 June 1999; accepted 30 July 1999)

Abstract—Photoinduced electron transfer of C₆₀ has been studied by the laser photolysis measuring the transient absorption bands in near-IR region. The electron transfer from aromatic amines *via* the triplet state of C₆₀ is confirmed by the decay of the transient absorption bands of the triplet state of C₆₀ and the rise of the anion radical of C₆₀ and the cation radicals of amines. The rate and efficiency of electron transfer are strongly affected by the donor ability of amines and polarity of solvents. Back electron-transfer kinetics is also strongly affected by the solvent polarity

INTRODUCTION

It has been well known that fullerenes act as good electron acceptors in photoinduced electron-transfer reaction, which attracts much attention in views of scientific and technological interests. In order to elucidate the electron-transfer mechanism, the transient absorption spectroscopies have been successfully employed.^{1–4} Because of highly delocalization of the π -electrons in fullerenes, the transient absorption bands due to the excited singlet states, triplet states, and anion radicals appear in the near-IR region.^{3–9}

As mechanism of photoinduced electron transfer of fullerenes, it is widely accepted that the excited states of fullerenes accept the electron from the electron-donors in their ground states.^{3,5–9} The relative contribution of the singlet states and the triplet states varies according to the experimental conditions. Since the intersystem crossing is as fast as 10⁹ s⁻¹,⁴ the singlet route can be achieved at high concentration of donors.^{3,5} At low concentration of donors, the triplet route is favorable.^{6–9}

We report here that the efficiency of the photoinduced elec-

tron transfer can be easily evaluated with the initial formation of anion radicals of fullerenes followed by the deactivation of their excited states. Especially, effect of solvent polarity on the electron transfer yields and rates is depending on the donor ability of aromatic amines employed in this study (Scheme 1).

In Scheme 1, E_{red} and E_{ox} refer to the reduction potential and oxidation potential vs. SCE in benzonitrile, respectively; T₁ to the lowest triplet energy.⁷

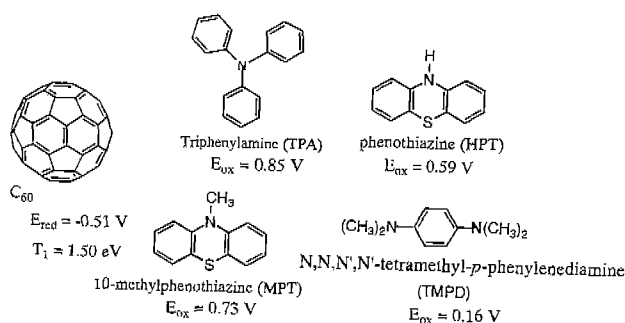
MATERIALS AND METHODS

Materials and Solvents. C₆₀ was obtained from Texas Fullerenes Corporation at a purity of 99.9%. Commercially available TMPD, PT, and TPA were used after purification by recrystallization. Benzonitrile (BN) and benzene (BZ) used as solvents were of HPLC grade and spectrophotometric grade, respectively.

Transient Absorption Measurements. Nanosecond laser photolysis apparatus was a standard design with Nd:YAG laser (6 ns fwhm). The C₆₀ solution was photolyzed with SHG light (532 nm) and the time profiles were followed by a photomultiplier system in the visible region. For the transient absorption measurement in the near-IR region, a germanium avalanche photodiode module (Ge-APD; Hamamatsu) attached to a monochromator was employed as a detector, using a pulsed Xe-lamp (60 μ s fwhm) for the probe light. The details of the experimental setup are described elsewhere.^{8,9}

Electrochemical measurements were made using a potentiostat (Hokuto Denko) in a conventional three-electrode-cell equipped with Pt working and counter electrodes and Ag/AgCl reference electrode with scan rates of 100 mV/s at room temperature. These data were converted to SCE standard.

The sample solutions were deaerated by bubbling with argon gas before measurements. The laser photolysis was performed



Scheme 1.

[†]To whom correspondence should be addressed.

for the solution in a rectangular quartz cell with a 10 mm optical path. All the measurements were carried out at 23°C.

RESULTS AND DISCUSSION

Fig. 1(a) shows the nano-second transient spectra of C_{60} in the visible and near-IR regions in the presence of TPA in polar BN solvent. The absorption band of $C_{60}^{\cdot-}$ appeared at 1070 nm with a decrease of ${}^3C_{60}^*$ at 750 nm. When the concentration of TPA is less than 5 mM, the decay rate of ${}^3C_{60}^*$ is in good agreement with the rise rate of $C_{60}^{\cdot-}$, indicating the electron transfer takes place *via* ${}^3C_{60}^*$. The absorption at 620 nm appeared after the decay of ${}^3C_{60}^*$ can be attributed to TPA $^{\cdot+}$.

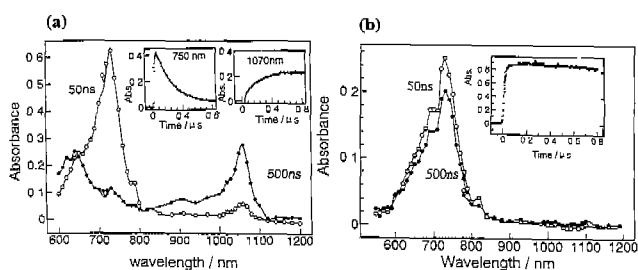


Figure 1. Transient absorption spectra obtained by ns-laser photolysis (532 nm) of C_{60} (0.1 mM) in the presence of TPA (1 mM); (a) in BN and (b) in BZ. Insert: Time profiles.

In non-polar BZ solvents, the appearance of $C_{60}^{\cdot-}$ was not observed and the decay rate of ${}^3C_{60}^*$ was not increased on addition of TPA as shown in Fig. 2(b). Further addition of TPA more than 50 mM, only slight increase in the decay rate of ${}^3C_{60}^*$ was observed, from which the quenching rate of ${}^3C_{60}^*$ by TPA in BZ was evaluated less than $10^5 \text{ M}^{-1} \text{ s}^{-1}$. In 1000–1100 nm region, no new absorption was observed.

The efficiency of the $C_{60}^{\cdot-}$ formation *via* ${}^3C_{60}^*$ was evaluated from the ratio of $[C_{60}^{\cdot-}]_{\text{max}}/[{}^3C_{60}^*]_{\text{max}}$ on substituting the molar extinction coefficient to the observed transient absorbance. Then, $[C_{60}^{\cdot-}]_{\text{max}}/[{}^3C_{60}^*]_{\text{max}}$ was plotted vs. [TPA] in various mixed solvents as shown in Fig. 2(a).

In each solvent, $[C_{60}^{\cdot-}]_{\text{max}}/[{}^3C_{60}^*]_{\text{max}}$ increases with [TPA] reaching to a plateau at about [TPA] = ca. 4 mM. The $[C_{60}^{\cdot-}]_{\text{max}}/[{}^3C_{60}^*]_{\text{max}}$ value at the plateau was defined as the quantum yield (Φ_{et}) of electron transfer *via* ${}^3C_{60}^*$. The Φ_{et} value for TPA is less

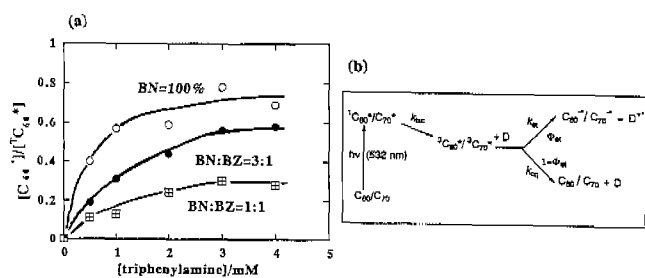


Figure 2. (a) $[C_{60}^{\cdot-}]/[{}^3C_{60}^*]$ vs. [TPA] in BN and BZ mixtures. (b) Reaction scheme.

Table 1. ${}^3C_{60}^*$ -quenching rate constants (k_q), quantum yield for electron transfer *via* ${}^3C_{60}^*$ (Φ_{et}), and electron-transfer rate constant (k_{et}).

Amines	Solvent	k_q $\text{M}^{-1}\text{s}^{-1}$	Φ_{et}	k_{et} $\text{M}^{-1}\text{s}^{-1}$
TMPD	BN	6.3×10^9	1.00	6.3×10^9
TMPD	BN:BZ	6.4×10^9	0.78	5.0×10^9
TMPD	BZ	1.2×10^9	0.19	2.3×10^9
PTH	BN	4.5×10^9	0.70	3.2×10^9
PTH	BN:BZ	5.2×10^9	0.50	2.6×10^9
PTH	BZ	4.5×10^9	0.06	2.6×10^8
MPTH	BN	3.2×10^9	0.70	2.2×10^9
MPTH	BN:BZ	7.6×10^9	0.50	3.8×10^9
MPTH	BZ	3.2×10^9	0.40	1.3×10^8
TPA	BN	1.3×10^9	0.63	8.2×10^9
TPA	BN:BZ	6.4×10^9	0.30	1.9×10^8
TPA	BZ	-	-	-

BN:BZ (1:1)

than 1, which implies that there are at least two route for the quenching of ${}^3C_{60}^*$ in polar solvents as shown in Fig. 2(b). One is electron transfer and another is deactivation process probably due to CT-interaction. The Φ_{et} values decrease with decreasing the solvent polarity, finally zero in non-polar BZ.

Fig. 2(b) indicated that the bimolecular quenching rate constants (k_q) evaluated from the ${}^3C_{60}^*$ -decay are not always equal to the rate constants for electron transfer *via* ${}^3C_{60}^*$ (k_{et}). Thus, the following relation, $k_{\text{et}} = \Phi_{\text{et}} \times k_q$,⁶ must be applied to the reaction scheme in Fig. 2(b), because k_q contains both k_{et} and the rate constant of collisional quenching (k_{eq}) without electron transfer. This suggests that a part of ${}^3C_{60}^*$ is deactivated without electron transfer ($1 - \Phi_{\text{et}}$) even in polar solvent.^{6,10} Since Φ_{et} increases with solvent polarity (Fig. 2(a)), the charge separation of the excited-triplet state encounter-complex (or triplet-state exciplex) is accelerated in the polar solvent.

In nonpolar solvent, deactivation processes of ${}^3C_{60}^*$ by TPA does not occur at all, indicating $\Phi_{\text{et}} = 0$ ($\Phi_{\text{dec}} = 1 - \Phi_{\text{et}} = 1$). At the low concentration condition of TPA in this study, fast electron transfer *via* singlet state exciplex or *via* ${}^1C_{60}^*$ was not necessary to take into consideration.

In the case of MPTH/ C_{60} , electron transfer was observed in BN, since the considerable amount of $C_{60}^{\cdot-}$ was formed with the decay of ${}^3C_{60}^*$ (Fig. 3(a)). The rise of the absorption band at 520 nm was attributed to MPTH $^{\cdot+}$. In BZ, although the acceleration of the decay of ${}^3C_{60}^*$ was observed in the same extent to that in BN, only small amount of $C_{60}^{\cdot-}$ was observed (Fig. 3(b)).¹¹ The Φ_{et} value decreases with the decrease in the solvent polarity; on the contrary, some deactivation processes may be effective. Although the decay time-profiles of ${}^3C_{60}^*$ in BZ was similar to that in BN, the rise and decay of $C_{60}^{\cdot-}$ in BZ were quite different from those in BN. $C_{60}^{\cdot-}$ seems to decay within the lifetime of ${}^3C_{60}^*$, suggesting that back electron transfer is quite fast in BZ. In the 520 nm region, no clear absorption due to MPTH $^{\cdot+}$ was not observed in BZ on contrary to Ghosh's observation.¹¹ The decay at 520 nm can be rather attributable to ${}^3C_{60}^*$.

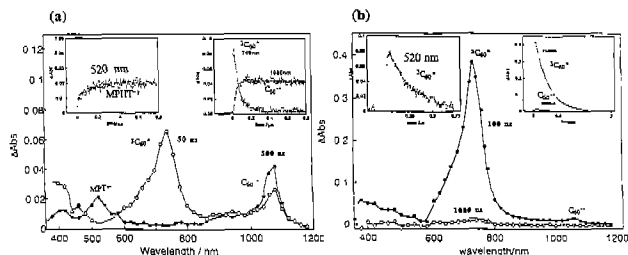


Figure 3. Transient absorption spectra obtained by ns-laser photolysis (532 nm) of C₆₀ (0.1 mM) in the presence of MPTH (1 mM) (a) in BN and (b) in BZ. Insert: Time profiles.

In the case of TMPD, the formation of C₆₀^{••} was observed both in polar and in nonpolar solvents, although the yield of C₆₀^{••} in nonpolar solvents was low compared with that in BN (Figs. 4(a) and (b)). The absorption band at 600 nm was attributed to TMPD^{•+} which appears clearly in BN. In BZ, the absorption band of TMPD^{•+} may be weak and broad overlapping with that of ³C₆₀^{*}. The decay time-profiles of ³C₆₀^{*} and C₆₀^{••} show very rapid in BZ. Since the decay rates of ³C₆₀^{*} increase with increasing [TMPD] from 1 to 5 mM, it is possible to ascribe the electrontransfer mechanism to the ³C₆₀^{*}-route even in BZ. At such a low concentration range of TMPD, it is difficult to consider that electron transfer takes place *via* the singlet route or *via* singlet-state exciplex route in nonpolar solvent.

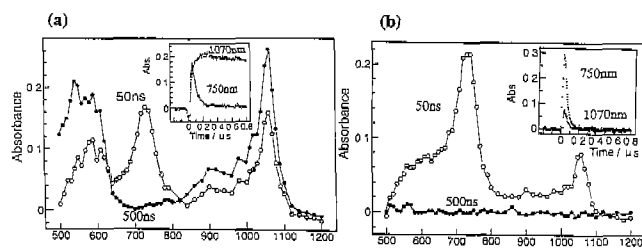


Figure 4. Transient absorption spectra obtained by ns-laser photolysis (532 nm) of C₆₀ (0.1 mM) in the presence of TMPD (1 mM) (a) in BN and (b) in BZ. Insert: Time profiles.

The ratio of [C₆₀^{••}]_{max}/[³C₆₀^{*}]_{max} increases with [TMPD], but not reaches to a plateau even at about [TMPD] = *ca.* 4 mM as shown in Fig. 5(a). In BN $\phi_{et} = 1$, indicating that all ³C₆₀^{*} are converted to C₆₀^{••} at [TMPD] = 4 mM. The ϕ_{et} value decreases with a decrease in solvent polarity, but even in BZ, the ϕ_{et} value has such a high value as *ca.* 0.4. The ϕ_{et} values are plotted vs. BZ-fraction in BN-BZ mixture as shown in Fig. 5(b). In every solvent mixture, the ϕ_{et} values are in the order of TMPD > MPTH > TPA. This order is in good agreement with the electron donor ability of these amines as presumed from the E_{ox} values in Scheme 1.

The k_{et} values are plotted vs. the solvent polarity as shown in Fig. 6(a). In the case of TMPD, the k_{et} values seem to be invariant with solvent polarity, while the k_{et} values for MPTH decrease with an increase in the BZ-fraction of BZ-BZ mixture. For TPA, the slope becomes steeper; at 100% BZ, the

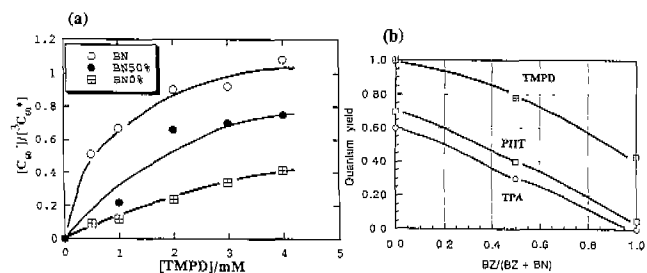


Figure 5. (a) [C₆₀^{••}]/[³C₆₀^{*}] vs. [TMPD] in BN and BZ mixtures. (b) Quantum yield vs. BZ/(BZ+BN).

k_{et} values in too low to evaluate. To interpret this tendency, a relation of $\log k_{et}$ vs. free energy change for electron transfer (ΔG^0) is illustrated by a curve anticipated from a semi-empirical Rehm and Weller relation.¹² In the region of $\Delta G^0 \ll 0$, the k_{et} value is close to diffusion controlled limit (k_{diff}); the k_{et} value does not change much with an decrease in solvent polarity. In the region of $\Delta G^0 = 0$, the k_{et} value decrease along the downward curvature with the decrease in solvent polarity. In the region of $\Delta G^0 \gg 0$, the downward curvature increase; thus, the large decrease in the k_{et} values can be expected along the steep curvature with a decrease in the solvent polarity.

Each ΔG^0 can be calculated by equation (1), where E_{ox}^D refers to oxidation potential of amine donor and E_{red}^A to reduction potential of acceptor (C₆₀) in BN. E_{T1} refers to the energy of the lowest triplet state of C₆₀ and a to the distance between ions.¹²

$$(\Delta G_{et}^0)_{in BN} = E_{ox}^D - E_{red}^A - E_{T1} - e_0^2/a\epsilon_{BN} \quad (1)$$

Since the E_{red}^A and E_{T1} for C₆₀ are common, ΔG^0 in BN increase toward negative value with a decrease in oxidation potential of amines as shown in Fig. 6b.

The ΔG^0 in the other solvents can be approximately evaluated as a solvent shift from (ΔG^0) in BN by eq. 2, where r_D and r_A refer to radii of donor and acceptor, respectively.

$$\Delta G_{et}^0 = (\Delta G_{et}^0)_{in BN} - e^2/2(1/r_D + 1/r_A)(1/\epsilon_{BN} + 1/\epsilon) \quad (2)$$

The values of the second term changing with the solvent from BN to BN:BZ (1:1) are less than *ca.* 5 kcal/mol. With this solvent change, the variation of the k_{et} values is small for most amines except for TPA, which stay near $\Delta G^0 = 0$. In BZ, ΔG^0 shifts more than *ca.* 25 kcal/mol to positive. For the electron-transfer process having sufficiently negative ΔG^0 such as TMPD, even such large shift of ΔG^0 to positive value with the decrease in the solvent polarity does not affect the k_{et} values much. On the other hand, amine with weak donor ability having $\Delta G^0 = 0$, large shift of ΔG^0 to the positive in less polar solvent causes the considerably drop of the k_{et} values.

Actual plots for $\log k_{et}$ vs. ΔG^0 are shown in Fig. 7. The reasonable decrease of the k_{et} values from BN to BN:BZ (1:1) is seen for TPA in the ΔG^0 region of -5 kcal/mol. Further drop of the k_{et} values going from BN to BZ would be anticipated, although it was difficult to measure such slow reaction by our laser flash photolysis apparatus. For other amine donors such as PHT and MPHT, the dots in BZ shift to more

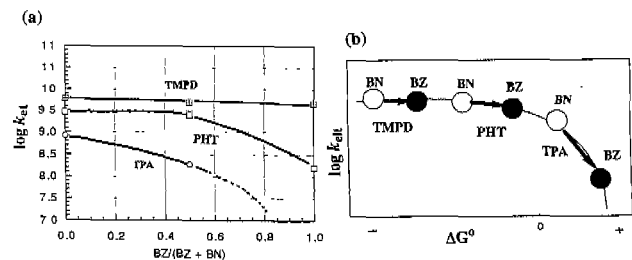


Figure 6. (a) Plots of $\log k_{et}$ vs. $BZ/(BZ+BN)$. (b) Schematic representation of solvent polarity effect on k_{et} along the Rehm-Weller curve.

positive than the calculated lines. It is frequently pointed out that the ΔG° values are overestimation to much positive values by *ca.* 10 kcal/mol.¹² Thus, the dots in BZ should be pushed back to negative as indicated by arrows in Fig. 7; the dots are in good agreement to the lines.

In Fig. 7, two lines are depicted on the basis of the Rehm-Weller and Marcus theory. In addition to the k_{et} value for tetrakis(dimethylamino)ethylene with very low E_{ox}^D ,¹³ drop of the k_{et} value in large negative ΔG° region was not observed, indication that the Rehm-Weller relation is more appropriate for such $C_{60}^{\cdot-}$ and amine systems in polar dilute solutions.

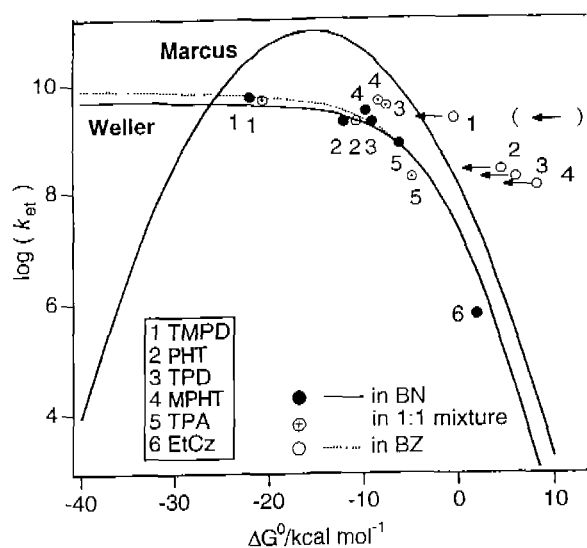


Figure 7. Plots of $\log k_{et}$ vs. ΔG° along the calculated curves with the Rehm-Weller and Marcus equations. TPD (N,N-diphenyl-N,N-bis(2,4-dimethylphenyl)-(1,1-biphenyl)-(4,4-diamine) and EtCz(ethylcarbazole).

The decay process of $C_{60}^{\cdot-}$ gives a clue of the electron transfer mechanism and ionpair state of the ion radicals. In polar solvents, $C_{60}^{\cdot-}$ decays slowly with obeying second-order kinetics as shown in Fig. 8(a). This clearly indicates that the ion radicals produced by electron transfer are solvated into free ion radicals, which are decaying with back electron transfer in almost diffusion controlled limit. In BZ, the decay of $C_{60}^{\cdot-}$ was faster than those in polar solvents. $C_{60}^{\cdot-}$ decays obeying first-order kinetics, indicating that the back electron

transfer takes place within the contaction pair (Fig. 8(b)). In the BN:BZ solvent mixture, both the initial fast decay and latter slow decay were observed (Fig. 8(a)).

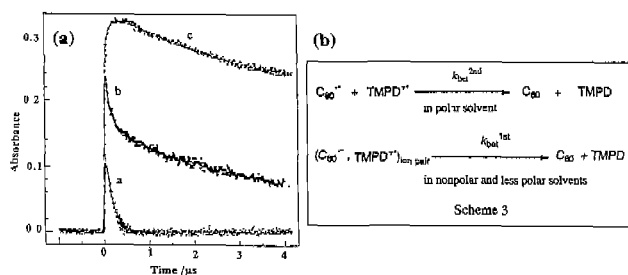


Figure 8. (a) Back electron transfer kinetics: a; first-order decay of $C_{60}^{\cdot-}$ in BZ; b; first- and second-order decay in BN:BZ (1:1) and c; second-order decay in BN. (b) Reaction scheme.

In the case of TMPD, the fractions of the fast (F_{fast}) and slow decay (F_{slow}) are summarized in Table 2 with the back electron-transfer rate constants for first-order (k_{bet}^{1st}) and second-order (k_{bet}^{2nd}). F_{fast} becomes prominent with increase in BZ in BN, especially when BZ is more than 70% in solvent mixture. In the region of BZ-rich solvent (BN% = 30-10%), both the first and second-order decay are present in the same solvent. This suggests that there are two distinct solvation states rather than an averaged-solvation state in each solvent mixture. This may be characteristic of $C_{60}^{\cdot-}$ having large round delocalized charge.

The k_{bet}^{2nd} value in BN is close to the diffusion controlled limit in BN. With the increase in the BZ fraction, the k_{bet}^{2nd} values seem to increase slightly, which is attributed to the decrease in the viscosity with an increase in BZ. The k_{bet}^{1st} values increase with BZ fraction, which indicates that the ion pair structure becomes more contact with an increase in nonpolar BZ. Kinetics analysis of back electron-transfer process with changing the solvent polarity affords quite valuable information of the ion radicals in solution.

Table 2. Decay of $C_{60}^{\cdot-}$ for the reaction with TMPD (F_{fast} , k_{bet}^{1st} , F_{slow} and k_{bet}^{2nd}) in BN and BZ mixture.

BN vol%	F_{fast} %	k_{bet}^{1st} s ⁻¹	F_{slow} %	k_{bet}^{2nd} M ⁻¹ s ⁻¹
100	0	— ^a	100	6.5×10^9
75	0	— ^a	(100)	6.0×10^9
50	0	— ^a	(100)	1.0×10^{10}
30	55	4.5×10^6	45	1.7×10^{10}
25	77	1.2×10^7	23	1.9×10^{10}
20	82	1.8×10^7	18	2.0×10^{10}
0	100	2.5×10^7	0	— ^b

- a) Decay of $C_{60}^{\cdot-}$ at 1070 nm band obeys almost completely second-order kinetics.
 b) Decay of $C_{60}^{\cdot-}$ at 1070 nm obeys almost completely first-order kinetics.
 c) The ϵ_{1070} nm value for $C_{60}^{\cdot-}$ employed in this calculation is reported value in BN.¹⁰

SUMMARY

The direct observation of both the transient absorption bands of ${}^3\text{C}_{60}^*$ and $\text{C}_{60}^{\cdot-}$ in addition to that of $\text{D}^{\cdot+}$ affords rich information about the photoinduced electron transfer and successive back electron-transfer processes. At low concentration of donors, electron transfer *via* ${}^3\text{C}_{60}^*$ takes place even in less polar solvents. Even in non polar solvents, electron transfer takes place when donor ability of donor is high.

Acknowledgments—The present work was partly supported by the Grant-in-Aid on General-Research B (No. 11440211) and Priority-Area-Research on "Laser Chemistry of Single Nanometer Organic Particle" (No. 10207202) from the Ministry of Education, Science, Sport and Culture.

REFERENCES

1. Arbogast, J. W., A. P. Darmany, C. S. Foote, Y. Robin, F. N. Diederich, M. M. Alvarez, S. J. Anz and R. L. Whetten (1991) Photophysical properties of C₆₀. *J. Phys. Chem.* **95** (11), 11-12.
2. Kajii, Y., T. Nakagawa, S. Suzuki, Y. Achiba, K. Obi and K. Shibuya (1991) Transient absorption, lifetime and relaxation of C₆₀ in the triplet state. *Chem. Phys. Lett.* **181** (2, 3), 100-104.
3. Sension, R. J., A. Z. Szarka, G. R. Smith and R. M. Hochstrasser (1991) Ultrafast photoinduced electron transfer to C₆₀^{*}. *Chem. Phys. Lett.* **185** (3, 4), 179-183.
4. Lee, M., O. -K, Song, J. -C. Seo, D. Kim, Y. D. Suh, S. M. Jin and S. K. Kim. (1992) Low-lying electronically excited states of C₆₀ and C₇₀ and measurement of their picosecond transient absorption in solution. *Chem. Phys. Lett.* **196** (3, 4), 325-329.
5. Palit, D. K., H. N. Ghosh, H. Pal, A. V. Sapre and J. P. Mittal (1992) Dynamics of charge transfer in the excited amine complexes of fullerenes C₆₀ and C₇₀. A picosecond laser flash photolysis study. *Chem. Phys. Lett.* **198** (1, 2), 325-329.
6. Biczok, L., H. Linschitz and R. I. Walter (1992) Extinction coefficients of C₆₀ triplet and anion radical, and one-electron reduction of the triplet by aromatic donors. *Chem. Phys. Lett.* **195** (4), 339-346.
7. Arbogast, J. W., C. S. Foote and M. Kao (1992) Electron transfer to triplet C₆₀. *J. Am. Chem. Soc.* **114** (6), 2277-2279.
8. Ito, O., Y. Sasaki, Y. Yoshikawa and A. Watanabe (1995) Solvent effect on photoinduced electron transfer between C₆₀ and tetramethylbenzidine studied by laser photolysis. *J. Phys. Chem.* **99** (24), 9838-9842.
9. Sasaki, Y., Y. Yoshikawa, A. Watanabe and O. Ito (1995) Solvent effect of photoinduced electron transfer between C₆₀ and 3,3',5,5'-tetramethylbenzidine studied by nanosecond laser photolysis. *J. Chem., Soc. Faraday Trans.* **91** (15), 2287-2290.
10. Alam, M. M., A. Watanabe and O. Ito (1997) Efficient photoinduced electron transfer between C₆₀ and tetrathiafulvalenes studied by nanosecond laser photolysis. *J. Photochem. Photobiol. A: Chemistry* **104** (1), 59-64.
11. Ghosh, H. N., D. K. Palit, A. V. Sapre and J. P. Mittal (1997) charge separation, charge recombination and electron transfer reactions in solutions of fullerene-C₆₀ and phenothiazines. *Chem. Phys. Lett.* **265**, 365-373.
12. Luo, C. M. Fujitsuka, C. -H. Huang and O. Ito (1998) Photoinduced electron transfer from N,N-dimethylaniline to pyrrolidinofullerenes; Emphasized substituent effects with solvent polarity change. *J. Phys. Chem. A* **102** (45), 8716-8721.
13. Fujitsuka, M., C. Luo and O. Ito (1999) Electron-transfer reactions between fullerenes (C₆₀ and C₇₀) and tetrakis-(dimethylamino)ethylene in ground and excited states. *J. Phys. Chem. A* **103** (3), 445-449.